DISPLACED MASS, DEPTH, DIAMETER, AND EFFECTS OF OBLIQUE TRAJECTORIES FOR IMPACT CRATERS FORMED IN DENSE CRYSTALLINE ROCKS

DONALD E. GAULT*

Max-Planck-Institut für Kernphysik, Heidelberg, Germany

(Received 17 April, 1972)

Abstract. Empirical formulae are presented for calculating the displaced mass, depth, diameter, and effects of oblique trajectories for impact craters formed in dense crystalline rocks. The formulae are applicable to craters with diameters from approximately 10^{-3}–10^3 cm that require, respectively, impact kinetic energies of approximately 10 to 10^{16} ergs for their formation. The experimental results are in poor agreement with Öpik's theoretical calculations and raise questions on the validity of his theoretical model.

1. Introduction

The impact of small meteoritic particles against rocks on the lunar surface – as well as asteroids, meteoroids, and other atmosphere-free bodies – is a primary erosion process which must be evaluated in order to unravel the influence of other environmental factors and the evolutionary history of the bodies. Although the size and shapes of the resultant craters are of interest, it is of particular interest to be able to calculate the mass of material removed per impact event as a necessary step in determining erosion rates and the long-term effects of the meteoritic bombardment as a comminution process.

In spite of an extensive literature devoted to the subject of hypervelocity impact phenomena (*e.g.*, Kinslow, 1970), most of the literature is devoted to impacts into metals. There is little data that is concerned specifically with cratering in rocks and there has been, therefore, a limited basis for calculating the important parameters for cratering in rocks. Rinehart (1950) and Partridge and Vanfleet (1958) performed pioneering experiments on cratering in rock, but they were primarily concerned with applying their results to the interpretation of large lunar structures and terrestrial features, in the latter category mainly the Barringer crater which at that time was one of the few generally accepted terrestrial impact craters. Maurer and Rinehart (1960) studied impacts into sandstone and granite and presented, for the first time it is believed, quantitative data on crater volumes and size. These first data, however, are open to question for quantitative purposes due to the use of a ballistic pendulum to ascertain the impact velocities; ejecta spewed out of craters contributes a spurious component of momentum (*e.g.*, Gault and Heitowit, 1965) and, hence, to an erroneous velocity determination.

Probably the first data directly applicable to evaluating erosion rates were presented

* Permanent address: Planetology Branch, NASA, Ames Research Center, Moffett Field, Calif, 94035, U.S.A.

The Moon **6** (1973) 32–44. *All Rights Reserved*

by Gault *et al.* (1963) for impacts into basalt and were subsequently given by Moore *et al.* (1965) in a more detailed and refined form. With the exception of Öpik's theoretical analysis of cratering in rocks, which is summarized in Öpik (1969), Comerford's (1967) experimental studies of microparticle erosion is the most recent and only other known addition to the subject.

The analysis presented by Moore *at al.* (1965) is of particular significance to applications under consideration because it clearly shows that there is a pronounced 'scale effect' attributable to a change in the effective strength of the target material with size of the crater. Gault (1969) pointed out that neglect of this scale effect can lead to order of magnitude errors in the calculated mass ejected per impact event (and erosion rates). The data available to Moore *et al.* was limited, however, to a range of projectile kinetic energies KE of about three orders of magnitude (approximately $10^{8.5}$ to $10^{11.8}$ ergs) and does not include the range of greatest interest for lunar erosion by micrometeoroids having KE less than, say, 10^7 ergs. (Gault *et al.*, 1972). In the intervening period of time, additional hypervelocity impact data have been developed that permit formulation of new empirical criteria for the ejected mass, depth, and diameter of craters formed in basalt and granite by impacts at normal and oblique incidence over a KE range from approximately 10–10^{12} ergs. These new criteria and a comparison of the empirical results with Öpik's theoretical model and calculations are presented in the following sections.

2. Sources of Data

The earlier analysis by Moore *et al.* (1965) was based on 38 impact experiments using Fe, Al, and polyethylene projectiles against basalt and granite targets at normal incidence. To these data are now added results from 62 new experiments including 36 for impacts with oblique trajectories. The bulk of these (59) are for Al and Pyrex projectiles into basalt and granite targets, while three 'experiments' have been derived from results reported by Comerford (1967). The basalt targets were sawed blocks of unweathered rock from Putnam Peak near Vacaville, California. Granite targets were headstone material obtained from an unknown location in the California Sierra Nevada mountains, and a 'Georgie Grey' granite as reported by Hörz (1969). Target densities for the basalts vary between 2.7 to 2.86 g/cm^3 while the granites ranged from 2.6 to 2.7 g/cm^3. New measurements (18) of the unconfined compressive strength of the basalt, using $2.5 \times 2.5 \times 5$ cm blocks, averaged 3 kb with a standard deviation of 0.63 kb and a maximum range from 1.5 to 3.75 kb. Estimated shear strength is 0.95 kb when the angle of internal friction is taken as 48°. Strengths of the granites were not measured, but they are believed to be similar to those for the basalt.

Comerford (1967) has presented data for microparticle impacts of silicon-carbide (SiC) projectiles against crystalline magnetite (Fe_3O_4) and SiC and Fe projectiles against the meteorite Indarch–"a black, enstatite chondrite, rather like basalt in appearance and strength". Although these data were obtained under conditions of multiple impacts (*i.e.*, sandblasting) rather than single events, results equivalent to single particle impacts can be derived from Comerford's data for the average mass loss per particle impact event. It is not possible, however, to extract dimensional data for the craters.

3. Results

Figure 1 presents data from 64 experiments for impacts at normal incidence in terms of the ejected mass M_e, the projectile kinetic energy KE, and the densities of the target

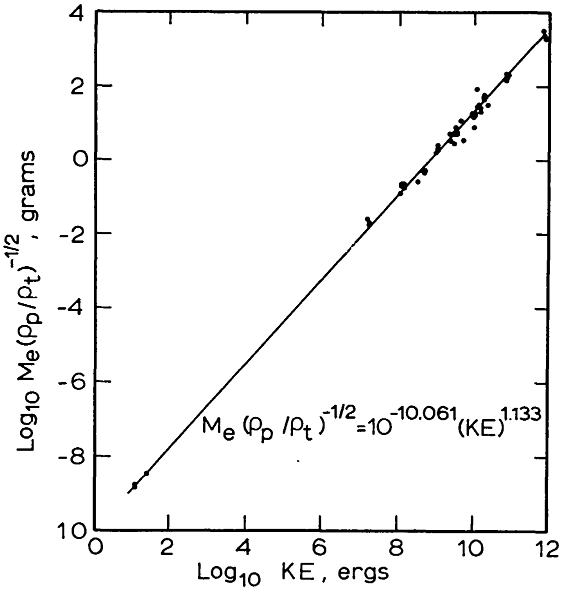

Fig. 1. Correlation of the displaced mass M_e (corrected for the effects of projectile-target density ratio) with the projectile kinetic energy KE. Impact at normal incidence to surface of target.

and projectile ρ_t and ρ_p, respectively. A least squares fit to these data was found, as shown on the figure, in the form

$$M_e = C_1\,[\varrho_p/\varrho_t]^{1/2}\,(\mathrm{KE})^{\delta} \tag{1}$$

with the constants C_1 and δ having values (cgs units)

$$\log_{10} C_1 = -\,10.061 \qquad \delta = 1.133$$

for which the confidence levels are

	$\log_{10} C_1$	δ
95%	± 0.185	± 0.018
99%	± 0.247	± 0.026

This relationship differs slightly from that given by Moore *et al.* (1965) in that the exponential term involves the KE and not the product of the KE and the density-ratio correction. This slight revision improves the correlation with respect to the original formulation given by Moore *et al.* (1965).

As originally pointed out by Moore *et al.* the slope of the correlation is significantly greater than 1.0 and is attributable to a change in the effective target strength with the dimensions of the masses of the target material that are engulfed and deformed by the stress waves produced by the impacts. It can be shown following the arguments given in Moore *et al.* (1965) using the Charters-Summers (1959) cratering theory that the value of δ depends on the mode of failure of the material fragmented and ejected from the craters. Failure solely in tension leads to $\delta = 1.2$ while compressive failure yields $\delta = 1.091$. The observed value of $\delta = 1.133$ suggests that both mechanisms of failure are important, but that tensile failure is probably the dominant process, consistent with the conclusions of Moore *et al.* (1961, 1965).

A least-squares fit for the depth p of the craters was found in the form

$$p = C_2 \varrho_p^{1/6} \varrho_t^{-1/2} (\mathrm{KE})^{\varepsilon}, \tag{2}$$

where the constants C_2 and ε have the values

$$\log_{10} C_2 = -3.450 \qquad \varepsilon = 0.357$$

with confidence levels of

	$\log_{10} C_2$	ε
95%	± 0.014	± 0.014
99%	± 0.018	± 0.019

Although the craters are approximately circular in planform, they are typically somewhat irregular in shape due to erratic spalling of the larger pieces of ejecta fragments. For this reason the crater diameter D_a has been taken to be the average of the maximum and minimum diameters. A least-squares fit yielded

$$D_a = C_3 \varrho_p^{1/6} \varrho_t^{-1/2} (\mathrm{KE})^{\lambda}, \tag{3}$$

with the constants C_3 and λ having values of

$$\log_{10} C_3 = -2.823 \qquad \lambda = 0.370$$

and the confidence levels are

	$\log_{10} C_3$	λ
95%	± 0.114	± 0.012
99%	± 0.155	± 0.016

Based on the form of Equations (2) and (3), the diameter-depth ratio D_a/p can be expressed as

$$D_a/p = C_4\,(\mathrm{KE})^{\tau}, \tag{4}$$

and a least-squares fit gave values for C_4 and τ of

$$\log_{10} C_4 = 0.615 \qquad \tau = 0.011$$

within the confidence limits of

	$\log_{10} C_4$	τ
95%	± 0.151	± 0.016
99%	± 0.205	± 0.022

A weak functional dependence of D_a/p with KE is indicated, but due to the erratic spalling causing relatively large statistical fluctuations in D_a the functional relationship is poorly defined. Combining Equations (2) and (3) directly yields equivalent values for $\log_{10}C_4$ and τ of, respectively, 0.617 and 0.013; the indicated trend for D_a/p to increase with increasing KE would seem to be real, but additional data will be necessary to improve the confidence levels of the functional relationships.

Finally, because the impact craters in the crystalline rocks are, to a first approximation, conical repressions with no raised rims (Moore *et al.*, 1961), a 'shape factor' C_5 can be derived by assuming that the crater volume V can be expressed

$$V = M_e/\varrho_t = C_5\left[\pi D_a^2 p\right] \tag{5}$$

A value for C_5 was found to be 0.084 with a standard deviation of 0.017. No systematic variation of C_5 with KE could be found.

It must be emphasized that the preceding correlations in Equations (1)–(5) include results for Fe, Al, Pyrex, SiC, and polyethylene projectiles ($\varrho_p = 7.8$–0.95 g/cm^3) into basalt, granite, magnetite, and the Indarch meteorite ($\varrho_t = 2.6$–5 g/cm^3) at normal incidence. The impact velocities range from 0.8–7.3 km s^{-1} with 85% between 2 and 7 km s^{-1}. Projectile masses vary from approximately 3×10^{-10} to 4 gr, and the KE varies from about 10–10^{12} ergs. Extrapolation of these results to higher velocities and events with greater KE should be done with knowledge of certain limitations. Hörz *et al.* (1971) have described microparticle impact craters up to a centimeter in diameter that they have observed on lunar rocks. The lunar craters characteristically exhibit a small, glass-lined pit centered in the spall zone which is typical of all the laboratory craters. Although there is ample evidence for shock melting in the laboratory experiments (Gault and Heitowit, 1963), the absence of the glass-lined pit in the laboratory may be due either to the lower velocity of the experiments and/or a scale effect. It is not known, however, whether or not the formation of the glass pit will cause any significant departures from the empirical relationships presented herein.

Extrapolation downward beyond KE = 10 ergs should be made very cautiously.

Evidence presented by Neukum *et al.* (1972) and Hartung *et al.* (1972) for microparticle craters formed in glasses indicates that the spall zone diminishes in size with decreasing size of the crater and eventually disappears for craters of the order of one micrometer in diameter, which corresponds to KE's of the order of one erg. Under such conditions the empirical relationships are probably not valid.

The formulae, however, probably may be safely extrapolated to larger KE. The author has observed craters formed in basalt and other brittle rocks by the detonations of TNT; these craters retain the characteristic conical shape of the laboratory features for explosive energy releases up to 10^{15}–10^{16} ergs. In the range of 10^{15}–10^{16} ergs, large spall-like plates of rock around the periphery of the craters, which at smaller scale are ejected from the craters, are apparently heaved upward with very low velocity only to settle down subsequently with small upward final displacements. This formation of incipient rims characteristic of large impact craters, marks a change in the crater geometry from the simple conical shape and negates the validity of the empirical formulae *for craters formed in a one 'g' gravitational field.* It is probable that in gravitational fields significantly lower than one '*g*' (*i.e.*, lunar and asteroidal), the large spall plates will eject from the crater. This could extend the use of the formulae to somewhat higher KE and larger craters, but such extrapolation beyond 10^{16} ergs is speculative and is not recommended.

4. Comparison with Öpik's Theory

It is important to compare these empirically derived results with the theoretical model and numerical results for cratering developed by Öpik. The reader is referred to Öpik (1969) for a detailed summary of the theory, and it is necessary here only to note that Öpik's model is based on the hypothesis that the cratering processes are a function only of the projectile momentum while, in contrast, the results presented herein have been related to the projectile KE. Öpik's relationship for M_e includes a 'constant' which varies with the impact velocity. This is a tacit inference that a strict momentum dependence is not correct, but the maximum variation in the constant is small (a factor of 2) and the difference between Öpik's theory and the present formulation is fundamental. To the author's knowledge, Öpik's theory has never been adequately compared previously with experimental data for hypervelocity impacts against rocks.

To compare Öpik's theoretical calculations with the experimental data, Figure 2 first presents results from both sources in terms of the displaced mass normalized with respect to the projectile mass M_e/m_p expressed as a function of the impact velocity V_i. It is to be emphasized that for this and subsequent comparisons, Öpik's theoretical values are based on a target density of 2.6 g/cm^3, a compressive strength of 2 kb, and a shear strength of 0.9 kb–values used by Öpik (1969) for stone and values that compare very closely to those for the basalt (and probably the granites) used in the experiments. The comparisons are, therefore, for cratering in materials with essentially identical physical properties and provide a valid test of Öpik's theory.

A least-squares fit to the experimental data shown in Figure 2 in the form

$$M_e/m_p = C_6 V_i^{\omega}$$

gives for the constants C_6 and ω

$$\log_{10} C_6 = -9.802 \qquad \omega = 2.117$$

within the confidence limits

	$\log_{10} C_6$	ω
95%	± 0.188	± 0.288
99%	± 0.250	± 0.383

In contrast, Öpik's formulation in the present terminology is

$$M_e/m_p = k\,(\varrho_t/s)^{1/2}\, V_i$$

where k is the velocity-dependent 'constant' and s is the shear strength. It can be seen that curve labeled Öpik (1969) in Figure 2, for which M_e/m_p varies essentially linearly with V_i based on the concept of momentum dependence, clearly fails to describe the trends or values of the experimental data, particularly for the highest velocities. On the other hand, the values obtained for ω indicate with strong statistical confidence that M_e/m_p is better described to vary with the square of the impact velocity. Thus, the experimental data substantiate the physical significance of KE in the cratering processes under consideration here and, at the same time, Figure 2

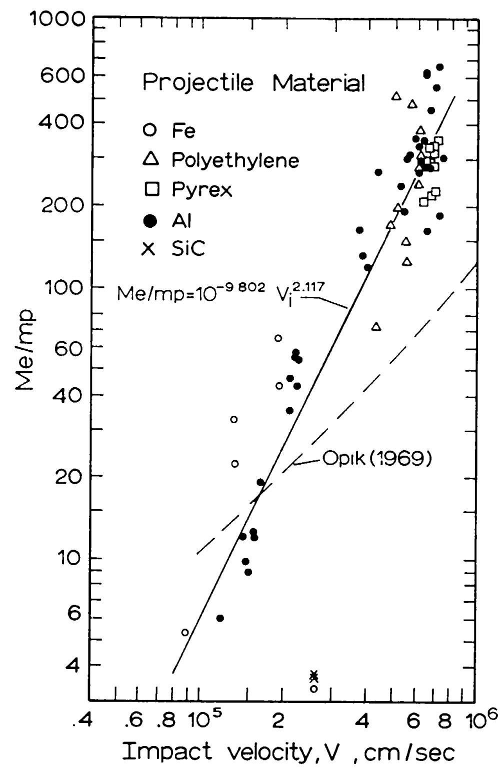

Fig. 2. Variation of the displaced mass M_e (normalized with the projectile mass m_p) with impact velocity V_i. Impact at normal incidence to surface of target.

confirms the correctness of the functional forms used in Equations (1), (2), and (3).

Additional comparisons between experiment and Öpik's theory can be made in regard to the effects of oblique trajectories on M_e, p, and D_a (values of D_a now become the average of the diameters measured along and at right angles to the track of the trajectory).

Figure 3 presents results for the effects of oblique impacts on the displaced mass M_e. For an impact angle i (measured with respect to the surface of the target) and all other parameters held constant, the displaced mass $(M_e)_i$ decreases with decreasing i from its value at normal incidence $(M_e)_{90}$. Although there is considerable experimental scatter in the data, the variation is well approximated by

$$(M_e)_i = (M_e)_{90} (\sin i)^2.$$

As shown in Figure 3, Öpik's theory predicts incorrectly that the displaced mass is independent of obliquity.

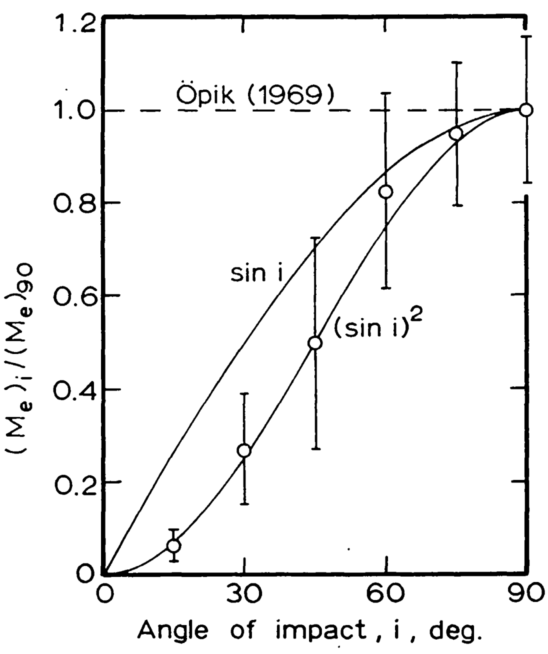

Fig. 3. Variation of the displaced mass $(M_e)_i$ with angle of impact i. Error bars are standard deviations.

Figures 4 and 5 present comparisons for the depth and diameter of craters formed by oblique impacts. Again the scatter is large, but it is clearly evident that both p and D_a decrease with decreasing values of i. The functional relationships cannot be defined with great confidence, but to a good approximation

$$p_i = p_{90} (\sin i)^m,$$
$$(D_a)_i = (D_a)_{90} (\sin i)^n,$$

with the exponents m and n having values between 1.0 and 2/3. Looking ahead, values of $m = 13/15$ and $n = 2/3$ are adopted. Öpik predicts $m = 1.0$ in agreement with

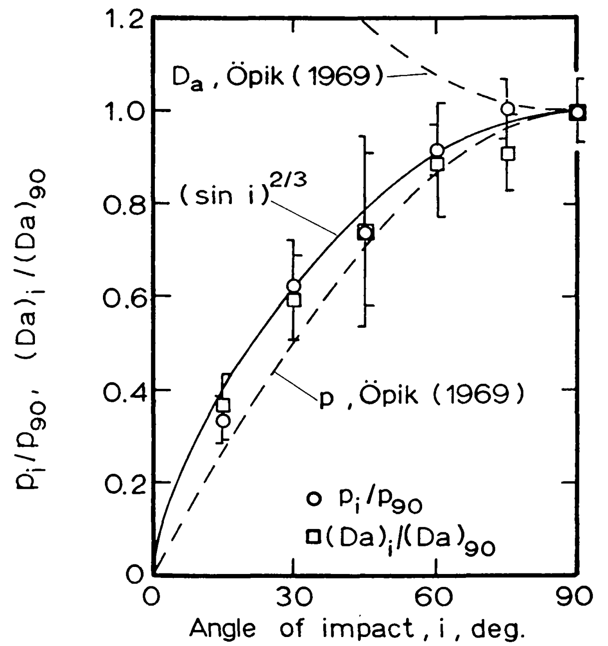

Fig. 4. Variation of crater depth p_i and crater diameter $(D_a)_i$ with angle of impact i. Error bars are standard deviations.

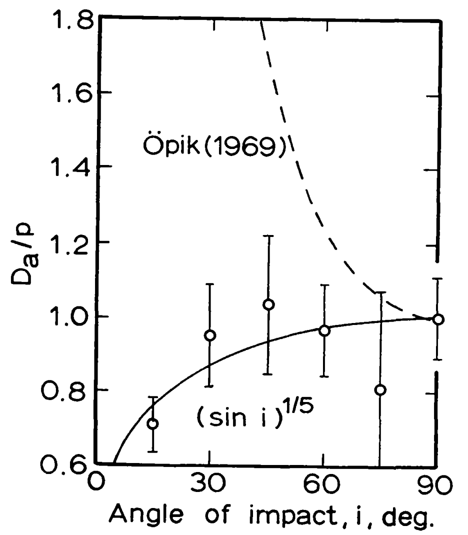

Fig. 5. Variation of crater diameter-depth ratio $(D_a/p)_i$ with angle of impact i. Error bars are standard deviations.

the experimental results, but he also predicts incorrectly that $n = -1/2$. This latter difference, as shown in Figure 5, leads to important differences between theory and experiment for the diameter–depth ratio D_a/p with decreasing values of i. Whereas the theory indicates that the craters will become larger in diameter and hence more shallow with increasingly oblique trajectories, the experimental results indicate that D_a/p remains approximately constant (or decreases very slowly) from normal incidence down to $i = 30°$ and then the ratio apparently decreases much more rapidly for obliquities less than $i = 15°$. If one uses the previous relationships for $(D_a/\mathrm{d})_i$ and p_i then

$$(D_a/p)_i = (D_a/p)_{90} (\sin i)^{n-m}$$

and the value for (n-m) must be rather small. Scatter in the data precludes, again, the evaluation of little more than a representative value (n-m)$=1/5$ as shown on Figure 5. Öpik's theory, however, predicts that (n-m)$=-3/2$ in complete contradiction to the experimental results.

For a final comparison, Equations (1), (2), and (3) for impacts at normal incidence are recast into dimensionless forms involving the projectile mass m_p and the diameter d of the spherical projectiles. With V_i the impact velocity

$$M_e/m_p = C_1 [\varrho_p/\varrho_t]^{1/2} (\mathrm{KE})^{\delta-1} (V_i^2/2), \tag{6}$$

$$p/\mathrm{d} = C_2 [\varrho_p/\varrho_t]^{1/2} (\mathrm{KE})^{\varepsilon-1/3} (\pi V_i^2/12)^{1/3}, \tag{7}$$

$$D_a/\mathrm{d} = C_3 [\varrho_p/\varrho_t]^{1/2} (\mathrm{KE})^{\lambda-1/3} (\pi V_1^2/12)^{1/3}. \tag{8}$$

Calculated values are compared in Table I with Öpik's theoretical results.

Inspection of the tabulation emphasizes that the theoretical calculations differ significantly from those from the empirically derived expressions. Of fundamental importance, Öpik's theory indicates neither the functional dependence of the parameters on KE nor the strong 'scale effect'. In general, Öpik's results overestimate the parameters M_e/m_p, p/d, and D_a/d for KE$=10$ ergs at the lower range of values of V_i, and the theoretical values grossly underestimate the parameters at 10^{11} and 10^{16} ergs for typical meteoritic velocities. In the intervening ranges of KE and V_i, of course, some agreement is attained.

The most direct and unbiased comparison of the validity of the theoretical calculations is to compare results for values of V_i and KE that were used in the laboratory experiments. Thus, for example, for $V_i=6$ km s^{-1} with KE$=10^{11}$ ergs and $\varrho_p=\varrho_t$ Öpik's calculated results for M_e/m_p are too low by a factor approaching an order of magnitude, p/d is low by about 40%, and D_a/d is underestimated by a factor greater than 2.5. When $\varrho_p=3\varrho_t$ that is representative for an iron projectile into stone targets, the differences for M_e/m_p, p/d, and D_a/d become, respectively, factors of 11, 1.4, and 3.3. Such differences cannot be attributed to either experimental errors or invalid extrapolations. Moreover, because the experimental data clearly indicate that KE rather than momentum is the important physical parameter to be used in describing the cratering processes, the use of Öpik's formulations has major ramifications for cratering at higher impact velocities and greater KE. For typical meteoritic impact velocities against the Moon (or Earth), say 20 km s^{-1}, the differences become greatly magnified and Öpik's calculations are consistently lower than values from the empirical formulation; that is, with $\varrho_p=\varrho_t$ for KE$=10^{16}$ ergs (corresponding to a terrestrial crater about 10 meters in diameter), Öpik predicts values of M_e/m_p lower by a factor of 126 with p/d and D_a/d being correspondingly lower by factors of 3.8 and 4.0, respectively.

Although the direct comparisons between theory and experiment can be made over

TABLE I

Cratering parameters calculated from the empirical formulae and Öpik's theoretical formulations for impacts at normal incidence

v_i, km s^{-1}	1	3	6	10	20	30	50	75	$\log_{10}$KE	Source
Stone projectile into stone target, $P_p = P_t = 2.6$ g/cm^3										
M_e/m_p	0.590	5.31	21.2	59.0	236	531	1470	3320	1	Equation (6)
	2.73	24.6	98.2	273.0	1090	2460	6820	15300	6	Equation (6)
	12.6	113.0	454.0	1260.0	5050	11300	31500	71000	11	Equation (6)
	58.3	525.0	2100.0	5830.0	28200	52500	146000	328000	16	Equation (6)
	10.8	32.7	69.0	127.0	224	666	1290	2000	–	Öpik [a]
p/d	0.517	1.07	1.71	2.40	3.81	4.99	7.01	9.19	1	Equation (7)
	0.681	1.42	2.25	3.16	5.02	6.58	9.25	12.1	6	Equation (7)
	0.898	1.87	2.97	4.17	6.12	8.67	12.2	16.0	11	Equation (7)
	1.18	2.46	3.91	5.50	8.72	11.4	16.1	21.1	16	Equation (7)
	1.88	2.03	2.12	2.20	2.30	2.37	2.45	2.51	–	Öpik [b]
D_a/d	2.26	4.69	7.45	10.5	16.6	21.8	30.6	40.1	1	Equation (8)
	3.45	7.18	11.4	16.0	25.4	33.3	46.9	61.4	6	Equation (8)
	5.29	11.0	17.5	24.5	39.0	51.1	71.8	94.1	11	Equation (8)
	8.10	16.8	26.7	37.6	59.7	78.2	110.0	144.0	16	Equation (8)
	2.88	4.82	6.86	9.12	14.8	20.2	27.6 [c]	33.9 [c]	–	Öpik [b]
Iron projectile into stone target, $P_p = 3$ g/cm^3, P_p 7.8 g/cm^3										
M_e/m_p	1.02	9.20	36.8	102.0	409	921	2560	5760	1	Equation (6)
	4.73	42.6	170.0	473.0	1890	4260	11800	26600	6	Equation (6)
	21.9	197.0	788.0	2190.0	8750	19700	54700	123000	11	Equation (6)
	101.0	910.0	3640.0	10100.0	40500	91000	253000	569000	16	Equation (6)
	10.8	33.1	71.3	137.0	401	727	1320	2010	–	Öpik
p/d	0.896	1.86	2.96	4.16	6.60	8.65	12.2	15.9	1	Equation (7)
	1.18	2.46	3.90	5.48	8.70	11.4	16.0	21.0	6	Equation (7)
	1.56	3.24	5.14	7.23	11.5	15.0	21.1	27.7	11	Equation (7)
	2.05	4.27	6.78	9.53	15.1	19.8	27.9	36.5	16	Equation (7)
	3.26	3.51	3.69	3.82	4.00	4.11	4.26	4.37	–	Öpik [b]
D_a/d	3.91	8.14	12.9	18.1	28.8	37.8	53.1	69.6	1	Equation (8)
	5.99	12.5	19.8	27.8	44.1	57.8	81.3	107.0	6	Equation (8)
	9.17	19.1	30.3	42.5	67.5	88.5	124.0	163.0	11	Equation (8)
	14.0	29.2	46.3	65.2	103.0	135.0	191.0	250.0	16	Equation (8)
	3.78	6.63	9.17	12.5	20.9	28.2	36.7 [c]	44.7 [c]	–	Öpik [b]

[a] Values calculated using Equation (10), Öpik (1969). [b] Values from Table II, Öpik (1969).

only the limited range of V_i and KE which are attainable in the laboratory, the available evidende strongly suggests that Öpik's model and numerical solutions are inadequate for describing the cratering processes quantitatively. Öpik's theory and numerical calculations, therefore, should be used with extreme caution for any impact cratering problems unless, possibly, supporting evidence can be found in the future for their validity for conditions of impact cratering differing from those considered herein (*i.e.*, different target materials, kilometer size craters, etc.):

Concluding Remarks

The results from 100 hypervelocity impact experiments indicate that the displaced mass M_e, the depth p, the average diameter D_a, and the diameter-depth ratio D_a/p of craters formed in basalt and granite may be calculated with the following empirically derived formulae:

$$\begin{aligned} M_e &= 10^{-10.061}\,[\varrho_p/\varrho_t]^{1/2}\,(\mathrm{KE})^{1.133}\,(\sin i)^2, \\ p &= 10^{-3.450}\varrho^{1/6}\varrho_t^{-1/2}\,(\mathrm{KE})^{0.357}\,(\sin i)^{0.66}, \\ D_a &= 10^{-2.823}\varrho_p^{1/6}\varrho_t^{-1/2}\,(\mathrm{KE})^{0.370}\,(\sin i)^{0.86}, \\ D_a/p &= 10^{0.617}\,(\mathrm{KE})^{0.013}\,(\sin i)^{0.2}, \end{aligned}$$

where cgs units are used throughout and where ϱ_p and ϱ_t are the density of the projectile and target, respectively, KE is the projectile kinetic energy, and i is the angle of the impacting trajectory measured with respect to the surface of the target (*i.e.*, $i=90°$ for normal incidence). These formulae are believed to be applicable to craters from approximately 10^{-3} to 10^3 cm in diameter that require approximately 10 to 10^{16} ergs, respectively, for their formation. Applications should be restricted to cases where the trajectory angle i is greater than about 15°.

Acknowledgements

B.C. Cour-Palais, NASA, Manned Spacecraft Center, and J. A. Wedekind, NASA, Ames Research Center, made important contributions to the new data used in the analysis. The support of the John Simon Guggenheim Memorial Foundation during preparation of the manuscript is gratefully acknowledged.

References

Charters, A. C. and Summers, J. L.: 1959, 'Some Comments on the Phenomena of High Speed Impact', NOLR 1238, U.S. Naval Ordnance Laboratory, White Oak, Silver Springs, Md., pp. 200–221.

Comerford, M. F.: 1967, *Geochim. Cosmochim. Acta* **31**, 1457–1471.

Gault, D. E., Shoemaker, E. M., and Moore, H. J.: 1963, 'Spray Ejected from the Lunar Surface by Meteoroid Impact', NASA TN D-1767.

Gault, D. E. and Heitowit, E. D.: 1963, *Proc. 7th Hypervel. Impact Symp.* **2**, pp. 419–456.

Gault, D. E.: 1969, Abstract in *Meteoritics* **4**, No. 3.

Gault, D. E., Hörz, F., and Hartung, J. B. 1972, 'Effects of Microcratering on the Lunar Surface', *Proc. 3rd Lunar Science Conf.*, in press.
Hörz, F.: 1969, *Contr. Min. Petrol.* **21**, 365–377.
Hörz, F., Hartung, J. B., and Gault, D. E.: 1971, *J. Geophys. Res.* **76**, 5770–5798.
Hartung, J. B., Hörz, F., McKay, D. S., and Baiamonte, F. L.: 1972, 'Surface Features on Two Glass Spherules from the Luna-16 Sample', *The Moon*, in press.
Kinslow, R. (ed.): 1970, *High Velocity Impact Phenomena*, Academic Press.
Maurer, W. C. and Rinehart, J. S.: 1960, *J. Appl. Phys.* **31**, 1247–1252.
Moore, H. J., Gault, D. E., and Lugn, R. V.: 1961, *Proc. 5th Hypervel. Impact Symp.* **1**, pp. 625–643.
Moore, H. J., Gault, D. E., and Heitowit, E. D.: 1965, *Proc. 7th Hypervel. Impact Symp.* **4**, pp. 35–45.
Neukum, G., Schneider, E., Mehl, A., Storzer, D., Wagner, G. A., Fechtig, H., and Bloch, M. R.: 1972, *Proc. 3rd Lunar Science Conf.*, in press.
Öpik, E. J.: 1969, *Ann. Rev. Astron. Astrophys.* **7**, 473–526.
Partridge, W. S. and Vanfleet, H. B.: 1958, *Astron. J.* **128**, 416–419.
Rinehart, J. S.: 1950, *Popular Astron.* **58**, 458–464.